doi:10.1016/j.jmb.2011.07.070 J. Mol. Biol. (2011) 412, 387–396

Contents lists available at www.sciencedirect.com

Journal of Molecular Biology

journal homepage: http://ees.elsevier.com.jmb

In Vitro Assembly of the øX174 Procapsid from External Scaffolding Protein Oligomers and Early Pentameric Assembly Intermediates

James E. Cherwa Jr[1,2]†, Lindsey J. Organtini[3], Robert E. Ashley[3], Susan L. Hafenstein[3] and Bentley A. Fane[1,2]*

[1]*School of Plant Sciences, University of Arizona, Tucson, AZ 85721, USA*
[2]*The BIO5 Institute, Keating Building, The University of Arizona, Tucson, AZ 85721-0240, USA*
[3]*Division of Infectious Diseases, Pennsylvania State University College of Medicine, Hershey, PA 17033-0850, USA*

Received 31 May 2011;
received in revised form
29 July 2011;
accepted 31 July 2011
Available online
5 August 2011

Edited by J. Karn

Keywords:
virus morphogenesis;
Microviridae;
microvirus

Bacteriophage øX174 morphogenesis requires two scaffolding proteins: an internal species, similar to those employed in other viral systems, and an external species, which is more typically associated with satellite viruses. The current model of øX174 assembly is based on structural and *in vivo* data. During morphogenesis, 240 copies of the external scaffolding protein mediate the association of 12 pentameric particles into procapsids. The hypothesized pentameric intermediate, the 12S* particle, contains 16 proteins: 5 copies each of the coat, spike and internal scaffolding proteins and 1 copy of the DNA pilot protein. Assembly naïve 12S* particles and external scaffolding oligomers, most likely tetramers, formed procapsid-like particles *in vitro*, suggesting that the 12S* particle is a *bona fide* assembly intermediate and validating the current model of procapsid morphogenesis. The *in vitro* system required a crowding agent, was influenced by the ratio of the reactants and was most likely driven by hydrophobic forces. While the system reported here shared some characteristics with other *in vitro* internal scaffolding protein-mediated systems, it displayed unique features. These features most likely reflect external scaffolding protein-mediated morphogenesis and the øX174 procapsid structure, in which external scaffolding–scaffolding protein interactions, as opposed to coat–coat protein interactions between pentamers, constitute the primary lattice-forming contacts.

Introduction

Bacteriophage øX174 morphogenesis combines features of seemingly disparate prokaryotic and eukaryotic viral systems. Capsid assembly involves the association of pentameric assembly intermediates,[1] a feature shared with polyoma, papilloma and picornaviruses.[2–5] However, as observed with many bacteriophages and herpesviruses,[6–9] morphogenesis requires scaffolding proteins to lower thermodynamic assembly barriers and ensure morphogenetic fidelity.[7,10] Most scaffolding-dependent systems utilize a single internal scaffolding protein, and the assembly-reactive coat protein is usually a monomer

*Corresponding author. The BIO5 Institute, Keating Building, The University of Arizona, Tucson, AZ 85721-0240, USA. E-mail address: bfane@email.arizona.edu.

Present address: J. E. Cherwa, Department of Microbiology, University of Alabama at Birmingham, Birmingham, AL 35294-2170, USA.

† All biochemical experiments were conducted at the University of Arizona. Electron microscopy and image reconstruction were performed at the Pennsylvania State University College of Medicine.

Abbreviations used: EDTA, ethylenediaminetetraacetic acid; PEG, polyethylene glycol; NIH, National Institutes of Health.

or a dimer, which does not display a defined stoichiometry with the scaffolding protein.[11–13] In contrast, the øX174 internal and external scaffolding proteins, B and D, respectively, exhibit strict stoichiometric relationships with the coat protein in both the procapsid and the early assembly intermediates.

Like the "classical" P22 and herpes simplex virus scaffolding proteins,[14,15] the øX174 B protein prevents coat protein aggregation and facilitates minor structural protein incorporation,[16–18] whereas protein D assembles pentameric intermediates into the procapsid (Fig. 1b). Viable multiple mutants that no longer require the internal scaffolding protein have been isolated.[19] Most of the mutations in this "*B-free*" strain affect the external scaffolding protein, its interactions with the viral coat protein and its expression level, which is grossly exaggerated. Along with the atomic structure of the procapsid, [20,21] these data indicate that the external scaffolding protein is more critical for morphogenesis. This may be a general feature of dual scaffolding protein systems. *In vitro*, the Sid protein, an external scaffolding protein encoded by satellite virus P4, can assemble P2 coat proteins into P4 procapsids,[22] circumventing the *in vivo* requirement of the P2 internal scaffolding protein. Despite this similarity, proteins D and Sid may operate via different mechanisms. The Sid protein alters capsid dimensions by forming a dodecahedral lattice that forces a growing coat protein shell into a smaller procapsid.[22–24] In contrast, the øX174 external scaffolding protein is the major lattice-forming molecule.[20,21,25] As can be seen in Fig. 1a, removing the external scaffolding protein density from the procapsid cryo-electron microscopy structure reveals underlying coat protein pentamers that make little or no contact with each other.[25] Thus, the coat protein pentamers act as a template on which external scaffolding proteins associate, but scaffolding–scaffolding interactions both form and maintain procapsid integrity.

Although *in vitro* capsid assembly systems have been established for many viruses,[2,3,12,13,22,26–32] the complexity of the øX174 procapsid has complicated *in vitro* reconstitution. Dissociation–reassociation studies were hindered by the heterogeneity of the dissociation products and the internal scaffolding protein's autoproteolytic activity.[25] Purifying proteins individually from cells expressing the requisite genes proved equally problematic. Consequently, an alternate strategy was developed. It utilized a recently isolated, putative, assembly intermediate that contains a stable internal scaffolding protein.[33]

The current version of the øX174 assembly pathway is illustrated in Fig. 1b. It differs from previous pathways[1,18,34] by the inclusion of two B protein-containing early intermediates, the 9S* and 12S* particles. These particles accumulate in the absence of the external scaffolding protein and can be easily purified.[33] The 12S* particle is composed of five copies each of the coat, spike and internal scaffolding proteins and one copy of the DNA pilot protein H. *In vitro*, it was assembled into procapsid-like particles by the external scaffolding protein, presumably in the form of a tetramer, suggesting that the 12S* particle is a *bona fide* assembly intermediate. While the assembly system reported here shared some characteristics with other *in vitro* scaffolding protein-mediated systems, it displayed unique features that most likely reflect external

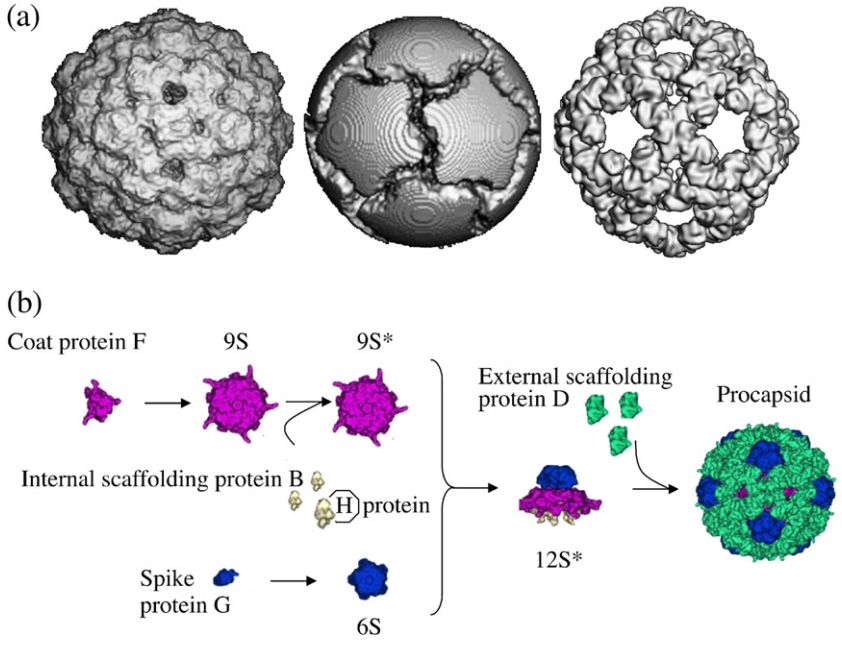

Fig. 1. Procapsid structures and assembly pathway. (a) Cryo-electron microscopy image reconstruction of the complete procapsid (left), density attributed to the coat protein pentamers (middle) and density attributed to the external scaffolding protein lattice (right). Figure courtesy of Drs. R. Bernal and M. G. Rossmann. (b) øX174 procapsid morphogenesis.

scaffolding protein-mediated morphogenesis and lattice formation.

Results

The external scaffolding protein used in the *in vitro* assembly reactions is most likely oligomeric

As described in Materials and Methods, the øX174 external scaffolding protein was purified from cells expressing a cloned wild-type gene. A large D protein band was evident in the whole-cell lysate analyzed by SDS-PAGE (data not shown). However, protein D exists in several oligomeric states in solution.[1,46,47] Therefore, whole-cell lysates and purified preparations were examined by native 7.5% polyacrylamide gel electrophoresis. Several novel bands were present in the whole-cell lysate (Fig. 2a). After purification, only one band was evident (Fig. 2b). As D protein's molecular mass is 16.9 kDa, the band's migration rate was most consistent with a tetramer. It is not known whether the utilized protocols selectively purified tetramers or the other oligomers were converted into this species during or after purification.

Procapsid-like particles can be assembled *in vitro* from pentameric 12S* intermediates and external scaffolding protein oligomers

The initial *in vitro* assembly reactions were performed with a 4.0% (w/v) polyethylene glycol (PEG)-3350 buffer under relatively low ionic conditions [2.5 mM NaCl, 9.0 mM $MgCl_2$ and 50 mM Tris–HCl (pH 7.5)]. The respective concentrations of the external scaffolding protein and 12S* particles were 0.24 mg/ml and 0.18 mg/ml. Mixed- and single-component reactions were simultaneously executed.

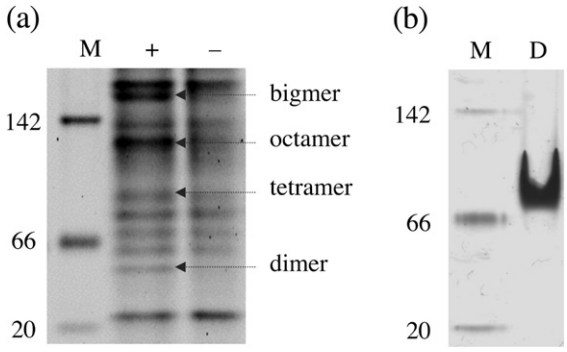

Fig. 2. The oligomeric state of the D protein before and after purification. (a) Native-PAGE of whole-cell lysates with (+) and without (–) the induction of the cloned D gene. (b) D protein after purification. M indicates the native molecular weight marker used as a standard.

Following a 40-min incubation at 37 °C, assembled particles were separated from unassembled components by rate-zonal sedimentation. After centrifugation, each 5.0-ml gradient was divided into approximately 40 fractions. Fractions were analyzed by UV spectroscopy (OD_{280}). For the single-component reactions (Fig. 3), no large particles were detected in the faster sedimenting fractions where procapsids (108S) and virions (114S) typically sediment. However, they were present in the fractions derived from the *in vitro* assembly reaction.

Gradient fractions were also examined by SDS-PAGE. No proteins were observed in the faster sedimenting fractions derived from the single-component reactions (data not shown). In contrast, all procapsid proteins were detected in the faster sedimenting fractions of the *in vitro* assembly reaction (Fig. 4a). Unassembled components remained at the top of the gradient, clearly separated from the more rapid sedimenting particles. The *in vitro* assembled procapsid-like particles and *in vivo* generated procapsids were examined by SDS-PAGE (Fig. 4b). The relative concentration of each protein was determined by densitometry. No significant differences between the two samples were detected (Table 1). To assay whether the *in vitro* assembled particles sediment like procapsids (108S), we added 1.0×10^4 infectious virions (114S), an amount that could be detected by neither SDS-PAGE nor UV spectroscopy, to a later reaction mixture as an internal *S*-value standard. After rate-zonal sedimentation, gradients were titered.

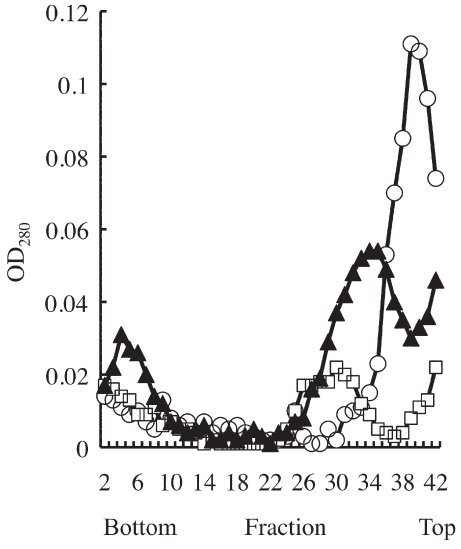

Fig. 3. Sedimentation profile of *in vitro* procapsid assembly and single-component reactions. Reaction products were separated by rate-zonal sedimentation as described in the text. Symbols: open circles, external scaffolding protein alone; open squares, 12S* particles alone; and filled triangles, 12S* particles and external scaffolding protein.

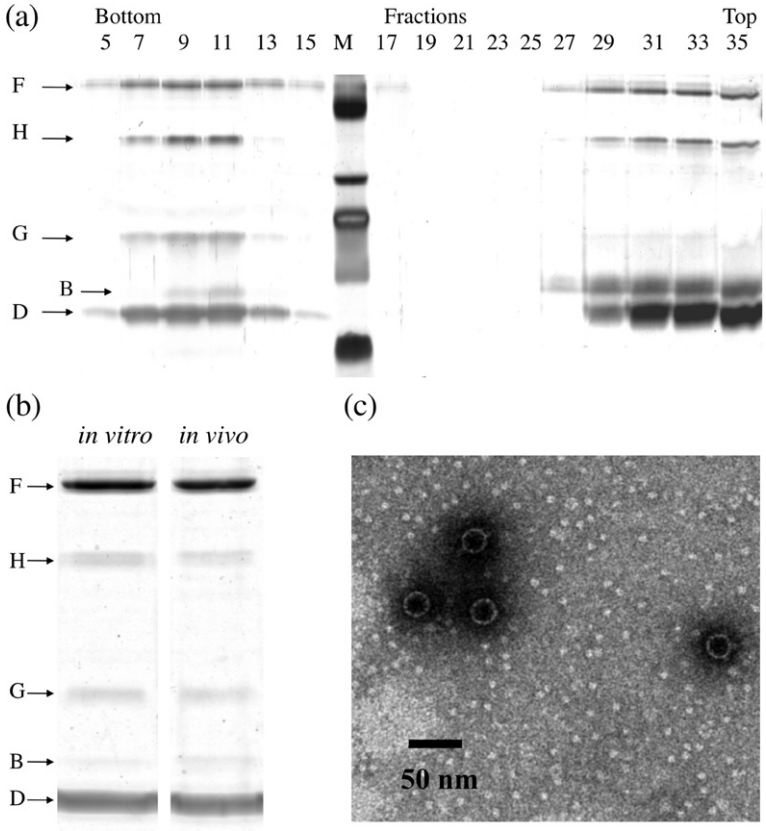

Fig. 4. Characterization of procapsid-like particles synthesized *in vitro*. (a) SDS-PAGE of gradient fractions of *in vitro* assembly reactions. Earlier fractions contain the faster sedimenting procapsid-like particles assembled *in vitro*. Later fractions contained unassembled components. Letters denote the viral proteins found in the procapsid: coat protein F, DNA pilot protein H, spike protein G, internal scaffolding protein B and external scaffolding protein D. (b) SDS-PAGE of *in vivo* and *in vitro* synthesized procapsids. (c) Electron micrograph of procapsid-like particles synthesized *in vitro*.

Infectivity roughly co-migrated with the *in vitro* synthesized particles (data not shown).

While electron micrographs of negatively stained, *in vitro* synthesized particles revealed spherical, stain-penetrated structures ~27 nm in diameter (Fig. 4c), a negative stain reconstruction was performed to more clearly demonstrate that the assembled particles were intact, not aberrantly shaped, and contained an external scaffolding protein lattice. The final resolution of the reconstruction was 23 Å. The presence of the phosphotungstic acid stain gives the *in vitro* assembled particles a more rounded appearance (Fig. 5a) compared to the low-resolution model calculated from the Protein Data Bank coordinates (Fig. 5b). However, the density of the spike protein pentamers and the external scaffolding protein lattice is clearly evident.

Table 1. Relative protein composition of procapsids synthesized *in vitro* and *in vivo*

	Relative protein ratios (protein:coat protein)	
Protein	*In vitro*	*In vivo*
Coat F	1.0	1.0
DNA pilot H	0.24	0.21
Major spike G	0.21	0.17
Internal scaffolding B	0.07	0.09
External scaffolding D	0.95	0.92

Digitized images of the gels presented in Fig. 4b were analyzed with NIH ImageJ software. The relative amount of each protein was determined by comparing the intensity of each protein band to the coat protein in each sample.

Crowding agents were essential for *in vitro* assembly

In optimizing the conditions, all experiments discussed here and below were conducted with the same preparation of 12S* particles and external scaffolding protein. To minimize any unforeseen problems associated with particle degradation, we performed all experiments within a 5-day time period. As no particles were observed migrating between *in vitro* assembled procapsids and unassembled components, the sedimentation profiles in Fig. 6 depict only the faster sedimenting fractions in which procapsids, if assembled, would be present.

As seen in other scaffolding-mediated *in vitro* assembly systems,[13,22,27,32] the concentration of the crowding agent significantly affected yields (Fig. 6a). No assembled particles were detected by UV spectroscopy of gradient fractions or SDS-PAGE followed by silver staining (data not shown) when the crowding agent PEG-3350 was omitted (black) or held at 2.0% (magenta). Increasing crowding agent concentrations resulted in progressively

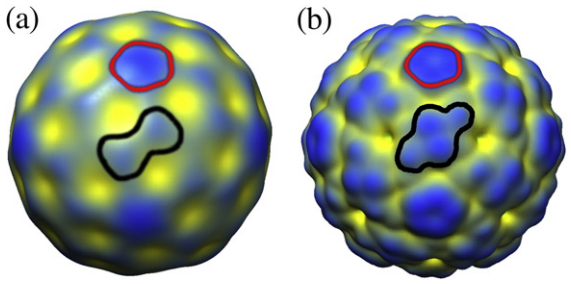

Fig. 5. Negative stain three-dimensional reconstruction of *in vitro* assembled procapsids. (a) Surface-rendered view of *in vitro* assembled procapsids. (b) Low-resolution model calculated from the X-ray crystal structure of øX174 procapsids. Regions composed of minor spike protein pentamers and the external scaffolding proteins are outlined in red and black, respectively. The reconstruction of the *in vitro* assembled particles has a more rounded, less defined surface due to the coating of negative stain.

higher yields (4.0%, orange; 8.0%, green; 10%, blue). No larger particles were detected in single-component reactions conducted in 10% PEG-3350 (red and turquoise). To estimate assembly efficiency, we digitized and analyzed silver-stained gels of all gradient fractions using the National Institutes of Health (NIH) ImageJ software. The percentages of assembled components are given in Table 2, lines 1–5. As the coat protein is the easiest component of the 12S* particle to visualize, it was used to follow 12S* particles. Due to the inherent error associated with conducting densitometry on multiple silver-stained gels, the values should be regarded as approximations that highlight trends in the data.

The external scaffolding:coat protein ratio strongly influences reaction yields

Unlike single-scaffolding protein assembly systems,[15,27,28,32,48] there are strict stoichiometric relationships between the coat and both scaffolding proteins. The external scaffolding:coat protein ratio in the procapsid is 4:1. This >1 ratio is unique to the øX174 procapsid. To determine how protein ratios affect assembly, we varied D protein concentrations. The 12S* particle and PEG-3350 (w/v) concentrations were held constant at 0.18 mg/ml and 10%, respectively. Although UV spectroscopy did not detect procapsids in gradient fractions derived from the 3:1 scaffolding:coat protein reaction (Fig. 6b, magenta), both proteins were visualized by SDS-PAGE and silver staining (data not shown). However, only ~5% of the coat protein was found in assembled particles (Table 2, lines 6–9). As the scaffolding:coat ratio increased, yields improved (Fig. 6b, in increasing order: orange, green and blue; Table 2, lines 6–9). In similar experiments, the 12S* concentration was varied, and the D protein concentration was held constant at 0.40 mg/ml (Fig. 6c and Table 2, lines 10–13). Assembled particles could be detected with a 12S* concentration as low as 0.045 mg/ml (Table 2, line 10).

In vitro assembly is relatively insensitive to ionic conditions

Ionic conditions are known to influence the efficiency of other scaffolding protein-mediated *in vitro* assembly reactions.[30,32,49] Optimal yields are usually obtained under low ionic conditions. To determine if the øX174 system exhibited a similar sensitivity, we examined yields as a function of NaCl concentrations between 2.5 and 80 mM. The respective concentrations of PEG-3350, external scaffolding protein and 12S* particles were 10% (w/v), 0.40 mg/ml and 0.18 mg/ml. As can be seen in Fig. 6d, *in vitro* assembly appears to be relatively insensitive within this NaCl concentration range, which is consistent with the nature of the interactions observed in the procapsid.[20,21]

Discussion

Several factors may have complicated past analyses of the early øX174 morphogenetic pathway. Consequently, the exact identities of the early intermediates have been somewhat obscure.[34] Procedural modifications led to the isolation of a novel assembly intermediate, the 12S* particle.[33] It consists of the coat, spike, internal scaffolding and DNA pilot proteins in a 5:5:5:1 ratio, a protein composition consistent with structural and genetic data.[18,20,21] Along with the external scaffolding protein, it can be assembled into procapsid-like particles *in vitro*, strongly suggesting that it is the *bona fide* assembly intermediate.

The external scaffolding protein, which has been observed in several oligomeric states in solution,[1,46,47] was purified from cells expressing a cloned gene. While several oligomers were observed in crude extracts, only one form, presumably a tetramer, was present after purification. Either this tetramer is the assembly-reactive species or the active form can be generated from it. Internal and external scaffolding protein oligomers have been observed in many viral systems.[27,28,50] The Sid protein, an external scaffolding protein, exists as a trimer in solution.[22] Bacteriophage P22 internal scaffolding protein dimers promote capsid nucleation, whereas monomers participate in elongation.[31]

As seen in other systems,[22,27,32] the crowding agent promoted efficiency. While it seemed to stimulate scaffolding–scaffolding interactions, it did not appear to promote coat–coat interactions between 12S* particles. In contrast, crowding agents promote bacteriophage ø29 coat–coat interactions

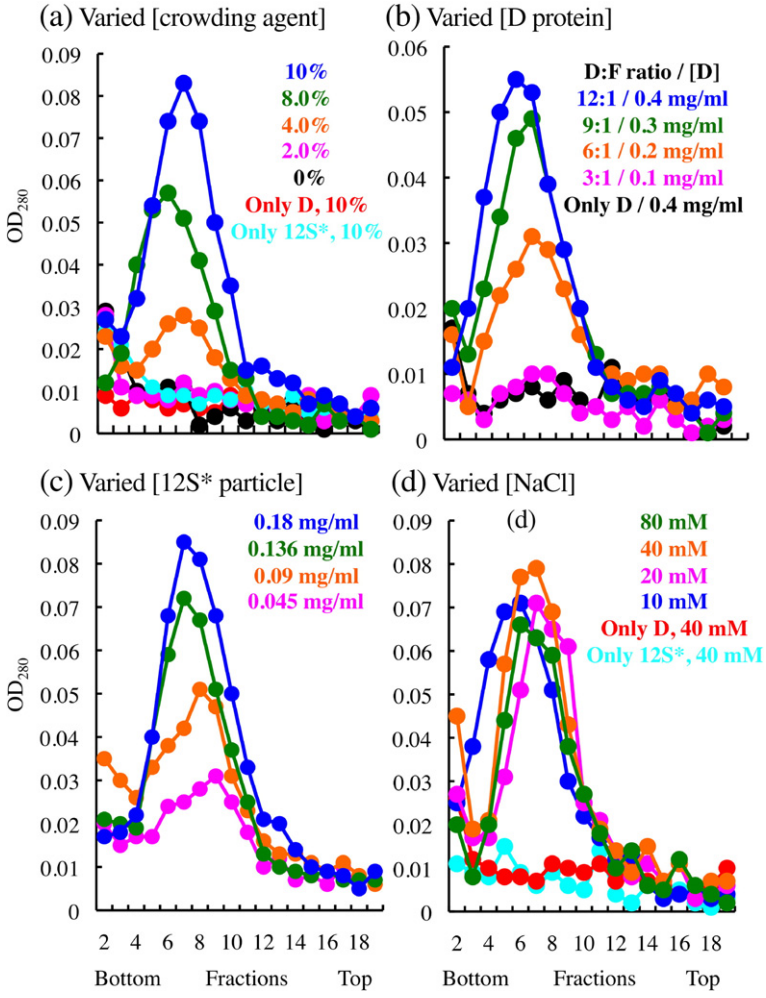

Fig. 6. Optimization of the *in vitro* assembly reaction. (a) Sedimentation profiles of *in vitro* assembly reactions conducted with varying concentrations (w/v) of the crowding agent PEG-3350. Crowding agent concentrations are given within the figure. The respective concentrations of the external scaffolding protein and 12S* particles were 0.24 mg/ml and 0.18 mg/ml. (b) Sedimentation profiles of *in vitro* assembly reactions conducted with varying concentrations of external scaffolding protein. The respective 12S* particle and PEG-3350 concentrations were held at 0.18 mg/ml and 10% (w/v). The external scaffolding protein:coat protein ratios (D:F) and external scaffolding protein concentrations are given within the figure. (c) Sedimentation profiles of *in vitro* assembly reactions conducted with varying concentrations of 12S* particles. The respective external scaffolding protein and PEG-3350 concentrations were held at 0.4 mg/ml and 10% (w/v). 12S* particle concentrations are given within the figure. (d) Sedimentation profiles of *in vitro* assembly reactions conducted with varying concentrations of NaCl. The respective 12S*, external scaffolding protein and PEG-3350 concentrations were held at 0.180 mg/ml, 0.4 mg/ml and 10% (w/v). NaCl concentrations are given within the figure.

but have little or no effect on the scaffolding protein.[27] This may reflect differences between the ø29 procapsid, in which coat–coat interactions constitute the primary lattice-forming contacts, and the øX174 procapsid, which is held together by the external scaffolding protein. The 2- and 3-fold related coat protein contacts observed in the øX174 virion structure[51,52] do not form until the external and internal scaffolding proteins dissociate from the procapsid. Scaffolding protein release allows pentamers to radially collapse around the genome. In addition to its role of mediating 12S* particle formation, the internal scaffolding protein B most likely prevents premature pentamer–pentamer interactions. In the absence of protein B, coat protein pentamers form intracellular aggregates.[18]

Although the analyses presented here lacked the kinetic component needed to determine critical concentrations and distinguish between nucleation and elongation phases, the reaction's sensitivity to external scaffolding:coat protein ratios may offer some limited insights. The scaffolding:coat protein ratio in the procapsid is 4:1. In the presence of excess external scaffolding protein (scaffolding:coat protein = 30:1), reactions conducted at the lowest 12S* particle concentration (0.045 mg/ml) resulted in ~90% coat protein assembly. Similar yields were achieved at 24:1, 18:1 and 12:1 ratios. However, in 3:1 and 6:1 reactions, the assembled coat protein values were 5.0 and 50%, respectively. At the lower ratios, the external scaffolding protein may have fallen below the critical concentration required to nucleate assembly, and/or kinetically trapped, partially formed procapsids were produced. If the latter, the trapped intermediates lack stability and degraded into unassembled components. Proteins were never detected within the intermediate sedimenting fractions, the position where stable, partially formed procapsids would be expected to migrate.

The øX174 *in vitro* reaction appeared to be relatively insensitive to ionic conditions. Salt concentrations high enough to inhibit other scaffolding protein-mediated reactions[22,27,30,32] had no observable effect on øX174 assembly. This suggests that the 12S* → procapsid transition may primarily be driven by hydrophobic interactions, which is consistent with the atomic structure of the external scaffolding

Table 2. Conditions and approximate efficiencies of *in vitro* assembly reactions

Sample	Final concentrations			Molar ratio	Approximate % assembled	
	PEG (w/v) (%)	D (mg/ml)	12S* (mg/ml)	D:coat	D	Coat
1	0	0.24	0.18	7:1	NAD	NAD[a]
2	2.0	0.24	0.18	7:1	NAD	NAD
3	4.0	0.24	0.18	7:1	31	63
4	8.0	0.24	0.18	7:1	41	73
5	10	0.24	0.18	7:1	41	76
6	10	0.1	0.18	3:1	26	5
7	10	0.2	0.18	6:1	44	51
8	10	0.3	0.18	9:1	49	73
9	10	0.4	0.18	12:1	45	92
10	10	0.4	0.045	30:1	30	>90[b]
11	10	0.4	0.090	24:1	32	88
12	10	0.4	0.135	18:1	45	89
13	10	0.4	0.180	12:1	48	83

[a] NAD, no assembly detected.
[b] ">" indicates an estimate as no protein was detected in the unassembled fractions.

protein lattice.[20,21] The vast majority of scaffolding–scaffolding protein interactions are hydrophobic in nature. Similarly, low ionic conditions did not impact assembly as they do during hepatitis B virus and papillomavirus assembly.[2,4,26] In the hepatitis B virus system, coat protein dimers exist in several conformations. Low ionic conditions favor conformations that are structurally incompatible with dimer–dimer interactions and by extension capsid assembly.[29] It is unlikely that all stages of øX174 assembly will display this insensitivity. The current system only investigates the 12S* → procapsid transition. Considering that most interactions between the coat and the spike protein pentamers are water mediated,[51,52] electrostatic forces are likely to play a more significant role in 12S* particle morphogenesis.

Materials and Methods

Escherichia coli cell lines, øX174 strains and plasmids

The øX174 mutant *am(C)S10*, which contains an amber codon at position 10 of gene C, was generated by site-directed mutagenesis as previously described.[35] It was used to generate procapsids *in vivo* (see below). The øX174 *nullD* strain, *øX174 D9 fs440*, was used to generate 12S* particles (see below). The strain contains a deletion (*D9*) of the first nine codons, nucleotides 396–419 in the genome sequence,[36] and a frame-shift mutation, a deletion of nucleotide 440. Its isolation was identical with that of *øX174 D9*, which has been previously described.[37] These two strains, which were isolated at the same time, differ only in the spontaneous *fs440* mutation. Stocks were prepared in BAF30 pDNco, a *recA* derivative of *E. coli* C122[38] containing an IPTG-inducible, wild-type D gene. To construct pDNco, we placed an NcoI site, containing a start codon, at the beginning of the gene using a mutagenic upstream primer during PCR reactions. The D gene in plasmid pND[33] served as a template. The downstream primer annealed to the multi-cloning site. PCR products were digested with NcoI and HindIII and ligated into pSE420 (Invitrogen) digested with the same enzymes. The C900 *E. coli* strain used to generate 12S* particles (see below) contains the *slyD* mutation, which confers resistance to E-protein-mediated lysis.[39] All plating and stock preparation protocols have been previously described.[40]

12S* particle synthesis and purification

For generation of 12S* particles, 100 ml of *E. coli* C900 (*slyD*) was grown to a concentration of 1.0×10^8 cells/ml in TKY broth (1.0% tryptone, 0.5% KCl and 0.5% yeast extract) at 37 °C. Immediately prior to infection, $MgCl_2$ and $CaCl_2$ were added to respective concentrations of 10 mM and 5.0 mM. Cells were infected with *øX174 D9 fs440* at a multiplicity of infection of 5.0 and incubated for 3 h. Infected cells were concentrated by centrifugation, and the resulting pellet was resuspended in 2.0 ml of 100 mM NaCl, 5.0 mM ethylenediaminetetraacetic acid (EDTA), 6.4 mM Na_2HPO_4 and 3.3 mM KH_2PO_4 (pH 7.0). Cell lysis was accomplished by adding egg white lysozyme (3.0 mg/ml) and incubating on ice for 30 min. After incubation, 20 µl $CHCl_3$ was added, and the reaction was incubated at 37 °C for 2.0 min, followed by sonication on ice for 8.0 min. Debris was removed by centrifugation (10 min at 16,000*g*). The resulting supernatant was concentrated to 200 µl in a Nanosep® centrifugal filter column (30-kDa cutoff). The extract was then loaded atop a 5–30% sucrose gradient (w/v) made in 100 mM NaCl, 5.0 mM EDTA, 6.4 mM Na_2HPO_4 and 3.3 mM KH_2PO_4 (pH 7.0). Gradients were spun at 108,000*g* for 16 h at 4 °C. After centrifugation, gradients were separated into approximately sixty 80-µl fractions. The location of the 12S* particle in the gradient was determined by SDS-PAGE analysis of fractions.

External scaffolding protein synthesis and purification

For generation of the external scaffolding protein, 1.5 l of TKY broth (without ampicillin) was inoculated with

15 ml of a fresh overnight of BAF30 pND.[33] The culture incubated for 2 h at 37 °C and then was transferred to room temperature. The cloned gene was then induced by IPTG (0.75 mM). The culture incubated, while shaking, for an additional 22 h at room temperature. Cells were concentrated by centrifugation and resuspended in 20 ml of 20 mM Tris–HCl, pH 8.0. Cell lysis was performed as described above but with the omission of the sonication step. Cell debris was removed by centrifugation (20 min at 10,000*g*).

Successive ammonium sulfate precipitations, starting at 20% saturation, were performed to determine the optimal conditions for external scaffolding protein isolation. After the addition of $(NH_4)_2SO_4$, samples were incubated at 4 °C for 4 h with gentle stirring. Precipitant was collected by centrifugation (20 min at 10,000*g*). Pellets were resuspended in 10 ml of 20 mM Tris–HCl (pH 8.0). Additional $(NH_4)_2SO_4$ was added to the supernatant, and the procedure was repeated. Successive precipitations were performed at 30%, 40%, 50% and 60% saturations. Protein D efficiently precipitated at 30% $(NH_4)_2SO_4$ saturation, as determined by SDS-PAGE. The resuspended 30% $(NH_4)_2SO_4$ pellet was dialyzed (3.5-kDa cutoff) against 700 ml of 20 mM Tris–HCl, pH 8.0, for 12 h at 4 °C. The dialyzed sample was spun for 20 min at 10,000*g* to remove remaining precipitant. Only D protein was detected by SDS-PAGE followed by Coomassie blue staining. By silver staining and subsequent densitometry, the protein was estimated to be 85–90% pure. Protein concentrations were estimated using a Bradford assay kit (Thermo Scientific) following the manufacturer's instructions.

Generation and purification of procapsids synthesized *in vivo*

For isolation of *in vivo* generated procapsids, 2 l of *E. coli* C900 (*slyD*) was grown to a concentration of 1.0×10^8 cell/ml at 37 °C. Cells were infected, as described above, with *am(C)S10* at a multiplicity of infection of 5. Protein C is essential for DNA packaging. Thus, procapsids accumulate in infected cells.[41] Particles were isolated and purified as previously described.[42]

In vitro assembly reactions and subsequent analyses

The 12S* particles and D protein were mixed with buffer [100 mM Tris–HCl (pH 7.5), 5 mM NaCl and 20 mM $MgCl_2$] pre-warmed to 37 °C. The final concentration of the buffering components was kept constant at 50 mM Tris–HCl, 2.5 mM NaCl and 9.0 mM $MgCl_2$ by the addition of H_2O and/or other components, PEG-3350 and/or NaCl, as needed. In experiments that varied NaCl and PEG-3350 concentrations, the final concentrations of these components are given in the text. Final reaction volumes were 200 μl. After incubation for 40 min at 37 °C, reactions were loaded atop a 5–30% sucrose (w/v) gradient made in 100 mM NaCl, 5.0 mM EDTA, 6.4 mM Na_2HPO_4 and 3.3 mM KH_2PO_4 (pH 7.0) and spun at 192,000*g* for 1 h. Gradients were divided into approximately forty 125-μl fractions and analyzed by UV spectroscopy (OD_{280}) and SDS-PAGE followed by Coomassie and silver staining.

Electron microscopy and image reconstruction

An aliquot of 3.0 μl of the *in vitro* procapsid sample was placed on a freshly glow-discharged continuous carbon-coated copper grid. Phosphotungstic acid negative stain was applied by standard drop method, and the sample was examined in a JEOL 1400 transmission electron microscope at 120 kV. For the three-dimensional reconstruction, 200 micrographs were collected with a Gatan Orius SC 1000 CCD camera with Digital Micrograph at a calibrated magnification of 22,510×. We selected 2032 *in vitro* particles (Fig. 4c) using e2boxer of EMAN2.[43] We used 2031 particles for the reconstruction. These numbers were taken directly from the log file generated by the computer program. For reasons unknown, one particle was omitted; it was not intentionally rejected. The defocus distance ranged from 0.07 to 4.34 μm. The final pixel size was 4.0 Å. The reconstruction processes were performed using icosahedral averaging with the program Auto3dem, which generated a random model directly from the raw data as the initial starting structure. The final resolution of 23 Å was determined where the Fourier shell correlation fell below 0.5 as reported in the summary output file of Auto3dem.[44] The final reconstruction was colored radially using the program Chimera.[45] The X-ray crystallography structure was calculated from the Protein Data Bank file, accession number 1CD3, using pdb2mrc.[43]

Acknowledgements

The authors thank Drs. R. Bernal and M. G. Rossmann for their assistance in generating Fig. 1a and Michael S. Carnegie for technical assistance. Molecular graphic images were produced using the University of California, San Francisco Chimera package from the Resource for Biocomputing, Visualization and Informatics at the University of California, San Francisco (supported by NIH P41 RR-01081). This work was supported by a grant from the NIH (AI07927) to S.H. and National Science Foundation (grant MCB 0948399) to B.A.F.

References

1. Tonegawa, S. & Hayashi, M. (1970). Intermediates in the assembly of phi X174. *J. Mol. Biol.* **48**, 219–242.
2. Casini, G. L., Graham, D., Heine, D., Garcea, R. L. & Wu, D. T. (2004). *In vitro* papillomavirus capsid assembly analyzed by light scattering. *Virology*, **325**, 320–327.
3. Mukherjee, S., Kler, S., Oppenheim, A. & Zlotnick, A. (2010). Uncatalyzed assembly of spherical particles from SV40 VP1 pentamers and linear dsDNA incorporates both low and high cooperativity elements. *Virology*, **397**, 199–204.
4. Mukherjee, S., Thorsteinsson, M. V., Johnston, L. B., DePhillips, P. A. & Zlotnick, A. (2008). A quantitative description of *in vitro* assembly of human papillomavirus 16 virus-like particles. *J. Mol. Biol.* **381**, 229–237.

5. Rombaut, B., Foriers, A. & Boeye, A. (1991). *In vitro* assembly of poliovirus 14 S subunits: identification of the assembly promoting activity of infected cell extracts. *Virology*, **180**, 781–787.
6. King, J. & Casjens, S. (1974). Catalytic head assembling protein in virus morphogenesis. *Nature*, **251**, 112–119.
7. Fane, B. A. & Prevelige, P. E., Jr (2003). Mechanism of scaffolding-assisted viral assembly. *Adv. Protein Chem.* **64**, 259–299.
8. Rixon, F. J. (1993). Structure and assembly of herpesviruses. *Semin. Virol.* **4**, 135–144.
9. Shore, D., Deho, G., Tsipis, J. & Goldstein, R. (1978). Determination of capsid size by satellite bacteriophage P4. *Proc. Natl Acad. Sci. USA*, **75**, 400–404.
10. Zlotnick, A. & Fane, B. A. (2010). Mechanisms of icosahedral virus assembly. In *Structural Virology* (Agbandje-McKenna, M. & McKenna, R., eds), pp. 180–202, Royal Society of Chemistry, London, UK.
11. Parker, M. H., Casjens, S. & Prevelige, P. E., Jr (1998). Functional domains of bacteriophage P22 scaffolding protein. *J. Mol. Biol.* **281**, 69–79.
12. Newcomb, W. W., Homa, F. L., Thomsen, D. R. & Brown, J. C. (2001). *In vitro* assembly of the herpes simplex virus procapsid: formation of small procapsids at reduced scaffolding protein concentration. *J. Struct. Biol.* **133**, 23–31.
13. Prevelige, P. E., Jr, Thomas, D. & King, J. (1993). Nucleation and growth phases in the polymerization of coat and scaffolding subunits into icosahedral procapsid shells. *Biophys. J.* **64**, 824–835.
14. Newcomb, W. W., Thomsen, D. R., Homa, F. L. & Brown, J. C. (2003). Assembly of the herpes simplex virus capsid: identification of soluble scaffold–portal complexes and their role in formation of portal-containing capsids. *J. Virol.* **77**, 9862–9871.
15. Weigele, P. R., Sampson, L., Winn-Stapley, D. & Casjens, S. R. (2005). Molecular genetics of bacteriophage P22 scaffolding protein's functional domains. *J. Mol. Biol.* **348**, 831–844.
16. Cherwa, J. E., Jr, Young, L. N. & Fane, B. A. (2011). Uncoupling the functions of a multifunctional protein: the isolation of a DNA pilot protein mutant that affects particle morphogenesis. *Virology*, **411**, 9–14.
17. Ruboyianes, M. V., Chen, M., Dubrava, M. S., Cherwa, J. E., Jr & Fane, B. A. (2009). The expression of N-terminal deletion DNA pilot proteins inhibits the early stages of phiX174 replication. *J. Virol.* **83**, 9952–9956.
18. Siden, E. J. & Hayashi, M. (1974). Role of the gene beta-product in bacteriophage phi-X174 development. *J. Mol. Biol.* **89**, 1–16.
19. Chen, M., Uchiyama, A. & Fane, B. A. (2007). Eliminating the requirement of an essential gene product in an already very small virus: scaffolding protein B-free oX174, B-free. *J. Mol. Biol.* **373**, 308–314.
20. Dokland, T., Bernal, R. A., Burch, A., Pletnev, S., Fane, B. A. & Rossmann, M. G. (1999). The role of scaffolding proteins in the assembly of the small, single-stranded DNA virus phiX174. *J. Mol. Biol.* **288**, 595–608.
21. Dokland, T., McKenna, R., Ilag, L. L., Bowman, B. R., Incardona, N. L., Fane, B. A. & Rossmann, M. G. (1997). Structure of a viral procapsid with molecular scaffolding. *Nature*, **389**, 308–313.
22. Wang, S., Palasingam, P., Nokling, R. H., Lindqvist, B. H. & Dokland, T. (2000). *In vitro* assembly of bacteriophage P4 procapsids from purified capsid and scaffolding proteins. *Virology*, **275**, 133–144.
23. Dokland, T. (1999). Scaffolding proteins and their role in viral assembly. *Cell. Mol. Life Sci.* **56**, 580–603.
24. Marvik, O. J., Dokland, T., Nokling, R. H., Jacobsen, E., Larsen, T. & Lindqvist, B. H. (1995). The capsid size-determining protein Sid forms an external scaffold on phage P4 procapsids. *J. Mol. Biol.* **251**, 59–75.
25. Bernal, R. A., Hafenstein, S., Olson, N. H., Bowman, V. D., Chipman, P. R., Baker, T. S. *et al.* (2003). Structural studies of bacteriophage alpha3 assembly. *J. Mol. Biol.* **325**, 11–24.
26. Ceres, P. & Zlotnick, A. (2002). Weak protein–protein interactions are sufficient to drive assembly of hepatitis B virus capsids. *Biochemistry*, **41**, 11525–11531.
27. Fu, C. Y., Morais, M. C., Battisti, A. J., Rossmann, M. G. & Prevelige, P. E., Jr (2007). Molecular dissection of ø29 scaffolding protein function in an *in vitro* assembly system. *J. Mol. Biol.* **366**, 1161–1173.
28. Newcomb, W. W., Homa, F. L., Thomsen, D. R., Trus, B. L., Cheng, N., Steven, A. *et al.* (1999). Assembly of the herpes simplex virus procapsid from purified components and identification of small complexes containing the major capsid and scaffolding proteins. *J. Virol.* **73**, 4239–4250.
29. Packianathan, C., Katen, S. P., Dann, C. E., 3rd & Zlotnick, A. (2010). Conformational changes in the hepatitis B virus core protein are consistent with a role for allostery in virus assembly. *J. Virol.* **84**, 1607–1615.
30. Parent, K. N., Doyle, S. M., Anderson, E. & Teschke, C. M. (2005). Electrostatic interactions govern both nucleation and elongation during phage P22 procapsid assembly. *Virology*, **340**, 33–45.
31. Tuma, R., Tsuruta, H., French, K. H. & Prevelige, P. E. (2008). Detection of intermediates and kinetic control during assembly of bacteriophage P22 procapsid. *J. Mol. Biol.* **381**, 1395–1406.
32. Wang, S., Chang, J. R. & Dokland, T. (2006). Assembly of bacteriophage P2 and P4 procapsids with internal scaffolding protein. *Virology*, **348**, 133–140.
33. Cherwa, J. E., Jr, Uchiyama, A. & Fane, B. A. (2008). Scaffolding proteins altered in the ability to perform a conformational switch confer dominant lethal assembly defects. *J. Virol.* **82**, 5774–5780.
34. Hayashi, M., Aoyama, A., Richardson, D. L. & Hayashi, N. M. (1988). Biology of the bacteriophage øX174. In *The Bacteriophages* (Calendar, R., ed.), vol. 2, pp. 1–71. Plenum Press, New York, NY.
35. Fane, B. A., Shien, S. & Hayashi, M. (1993). Second-site suppressors of a cold-sensitive external scaffolding protein of bacteriophage phi X174. *Genetics*, **134**, 1003–1011.
36. Sanger, F., Coulson, A. R., Friedmann, T., Air, G. M., Barrell, B. G., Brown, N. L. *et al.* (1978). The nucleotide sequence of bacteriophage phiX174. *J. Mol. Biol.* **125**, 225–246.
37. Uchiyama, A., Heiman, P. & Fane, B. A. (2009). N-terminal deletions of the phiX174 external scaffolding protein affect the timing and fidelity of assembly. *Virology*, **386**, 303–309.
38. Fane, B. A., Head, S. & Hayashi, M. (1992). Functional relationship between the J proteins of bacteriophages

phi X174 and G4 during phage morphogenesis. *J. Bacteriol.* **174**, 2717–2719.
39. Roof, W. D., Horne, S. M., Young, K. D. & Young, R. (1994). slyD, a host gene required for phi X174 lysis, is related to the FK506-binding protein family of peptidyl-prolyl cis–trans-isomerases. *J. Biol. Chem.* **269**, 2902–2910.
40. Fane, B. A. & Hayashi, M. (1991). Second-site suppressors of a cold-sensitive prohead accessory protein of bacteriophage phi X174. *Genetics*, **128**, 663–671.
41. Fujisawa, H. & Hayashi, M. (1977). Functions of gene C and gene D products of bacteriophage phiX174. *J. Virol.* **21**, 506–515.
42. Uchiyama, A. & Fane, B. A. (2005). Identification of an interacting coat-external scaffolding protein domain required for both the initiation of phiX174 procapsid morphogenesis and the completion of DNA packaging. *J. Virol.* **79**, 6751–6756.
43. Tang, G., Peng, L., Baldwin, P. R., Mann, D. S., Jiang, W., Rees, I. & Ludtke, S. J. (2007). EMAN2: an extensible image processing suite for electron microscopy. *J. Struct. Biol.* **157**, 38–46.
44. Yan, X., Sinkovits, R. S. & Baker, T. S. (2007). AUTO3DEM—an automated and high throughput program for image reconstruction of icosahedral particles. *J. Struct. Biol.* **157**, 73–82.
45. Pettersen, E. F., Goddard, T. D., Huang, C. C., Couch, G. S., Greenblatt, D. M., Meng, E. C. & Ferrin, T. E. (2004). UCSF Chimera—a visualization system for exploratory research and analysis. *J. Comput. Chem.* **25**, 1605–1612.
46. Farber, M. B. (1976). Purification and properties of bacteriophage phi X 174 gene D product. *J. Virol.* **17**, 1027–1037.
47. Morais, M. C., Fisher, M., Kanamaru, S., Przybyla, L., Burgner, J., Fane, B. A. & Rossmann, M. G. (2004). Conformational switching by the scaffolding protein D directs the assembly of bacteriophage phiX174. *Mol. Cell*, **15**, 991–997.
48. Prevelige, P. E., Jr, Thomas, D. & King, J. (1988). Scaffolding protein regulates the polymerization of P22 coat subunits into icosahedral shells *in vitro*. *J. Mol. Biol.* **202**, 743–757.
49. Cerritelli, M. E. & Studier, F. W. (1996). Assembly of T7 capsids from independently expressed and purified head protein and scaffolding protein. *J. Mol. Biol.* **258**, 286–298.
50. Chang, J. R., Spilman, M. S., Rodenburg, C. M. & Dokland, T. (2009). Functional domains of the bacteriophage P2 scaffolding protein: identification of residues involved in assembly and protease activity. *Virology*, **384**, 144–150.
51. McKenna, R., Ilag, L. L. & Rossmann, M. G. (1994). Analysis of the single-stranded DNA bacteriophage phi X174, refined at a resolution of 3.0 Å. *J. Mol. Biol.* **237**, 517–543.
52. McKenna, R., Xia, D., Willingmann, P., Ilag, L. L., Krishnaswamy, S., Rossmann, M. G. *et al.* (1992). Atomic structure of single-stranded DNA bacteriophage phi X174 and its functional implications. *Nature*, **355**, 137–143.